Colloid Polym Sci (2008) 286:1351–1360
DOI 10.1007/s00396-008-1905-z

ORIGINAL CONTRIBUTION

Interfacial behaviors of densely anchored hydrophilic oligomeric chains on silica microspheres

Xinhui Zhang · Liang Hong · Zhaolin Liu · Jim-Yang Lee

Received: 11 January 2008 / Revised: 4 June 2008 / Accepted: 20 June 2008 / Published online: 7 August 2008

Abstract This work studies the interfacial behaviors of a thickly grafted hydrophilic oligomeric layer on silica microspheres ($\overline{d} \cong 1\ \mu m$). The surface layer comprises the homopolymer or block-copolymer chains of sodium 4-styrenesulfonate (SSNa) and 4-vinylpyridine (4VP). Such a core-shell microspheric structure is constructed by the atom transfer radical polymerization method. Two types of block-copolymer chains are synthesized through reversing the chain growing sequence of PSSNa and P4VP blocks, a copolymer double layer is, therefore, generated. It is found that these two block-sequences produce rather different impacts on the chain–chain interaction patterns. Furthermore, the functional group type and the sequence of the grafted copolymer blocks influence the hydrodynamic volume of the particles in the designated dispersion media with different pH or polarity. More appealingly, the two types of double-layers exhibit very different roles in mediating ion (H^+ or Na^+) transport in the liquid medium where a substantially low content of the microspheres is present.

Keywords Atom transfer radical polymerization · Grafting · Interfacial phenomena

X. Zhang · L. Hong (✉) · J.-Y. Lee
Department of Chemical and Biomolecular Engineering,
National University of Singapore,
BLK E5 02-2, 4 Engineering Drive 4,
Singapore 117576, Singapore
e-mail: chehongl@nus.edu.sg

L. Hong · Z. Liu
Institute of Materials Research & Engineering,
Agency for Science, Technology and Research (A*STAR),
3 Research Link,
Singapore 117602, Singapore

Introduction

Design and synthesis of a chemically grafted polymer thin layer at the surface of a solid substrate has paramount technological implications in different combinatory chemical systems, such as protein separation by selective adsorption [1], electrophoretic deposition [2], immobilization of biomolecules [3], and functional additives to various polymer formulations [4, 5]. Among various chemical means developed by far to graft functional polymer chains to a solid surface, the atom transfer radical polymerization (ATRP) method is a unique one because by which the initiator for chain growth is attached to the surface of substrate and, thus, polymer chains can be grown solely from that surface [6]. The more appealing feature of this methodology is that it allows a precise control over the distribution of monomer units in the resulting polymer chains via the "living" radical mechanism. To date a variety of styrenic or/and acrylic polymer chains have been successfully grafted to insoluble substrates by ATRP [7–15]. A recent development is the growing of hydrophilic polymer chains, which bear sulfonate, carboxylate, hydroxyl, and amide pendant groups, on solid particles. The water-borne colloidal, rheological, and electrochemical behaviors of the resulting hard-core and soft-shell particles are of particular importance in several technological arenas [16–20]. Moreover, it is still of interest to explore the corresponding traits if the soft shell is composed of diblock copolymer chains in which the two blocks carry opposite charges.

With the aim of constructing such a double-charged layer on rigid particles, trisiloxyl(1,2-dibromoethyl) groups (→Si-$CHBrCH_2Br$) were anchored to the surface of silica microspheres as the initiating sites of ATRP. The monomers used include an anionic monomer, sodium 4-styrenesulfonate (SSNa), and a proton-acceptor monomer, 4-vinylpyridine

(4VP). Therefore, we achieved four types of grafting chains: the homopolymers of SSNa and 4VP and the block copolymers in which the sequence of PSSNa and P4VP blocks was swapped (Scheme 1).

Recently, only a few investigations have been conducted to examine the interfacial behavior of the hydrophilic (or electrolyte chains) polymer segments on SiO_2 particles in aqueous solution. Their focuses were on the effect of ionic strength and electrostatic interaction [21, 22]. As an effort to advance understanding of such a hybrid particle system, this work divulges the unique glass transition behaviors, diverse responses of hydrodynamic volume and ζ potential to the change of pH, and different solvating power in the selected dispersion solvents. Furthermore, ionic transport behavior of the counter ion H^+ or Na^+ of polymer electrolyte in a designated liquid medium, where a substantially low volume fraction ($\sim 1.0 \times 10^{-2}$%) of the above synthesized particles is dispersed, has been investigated. The motive for this investigation is to understand whether these particles can be eventually utilized as the specialty filler for several technologically important polymer electrolyte membranes (such as lithium-polyethylene oxide and Nafion®) to enhance ionic

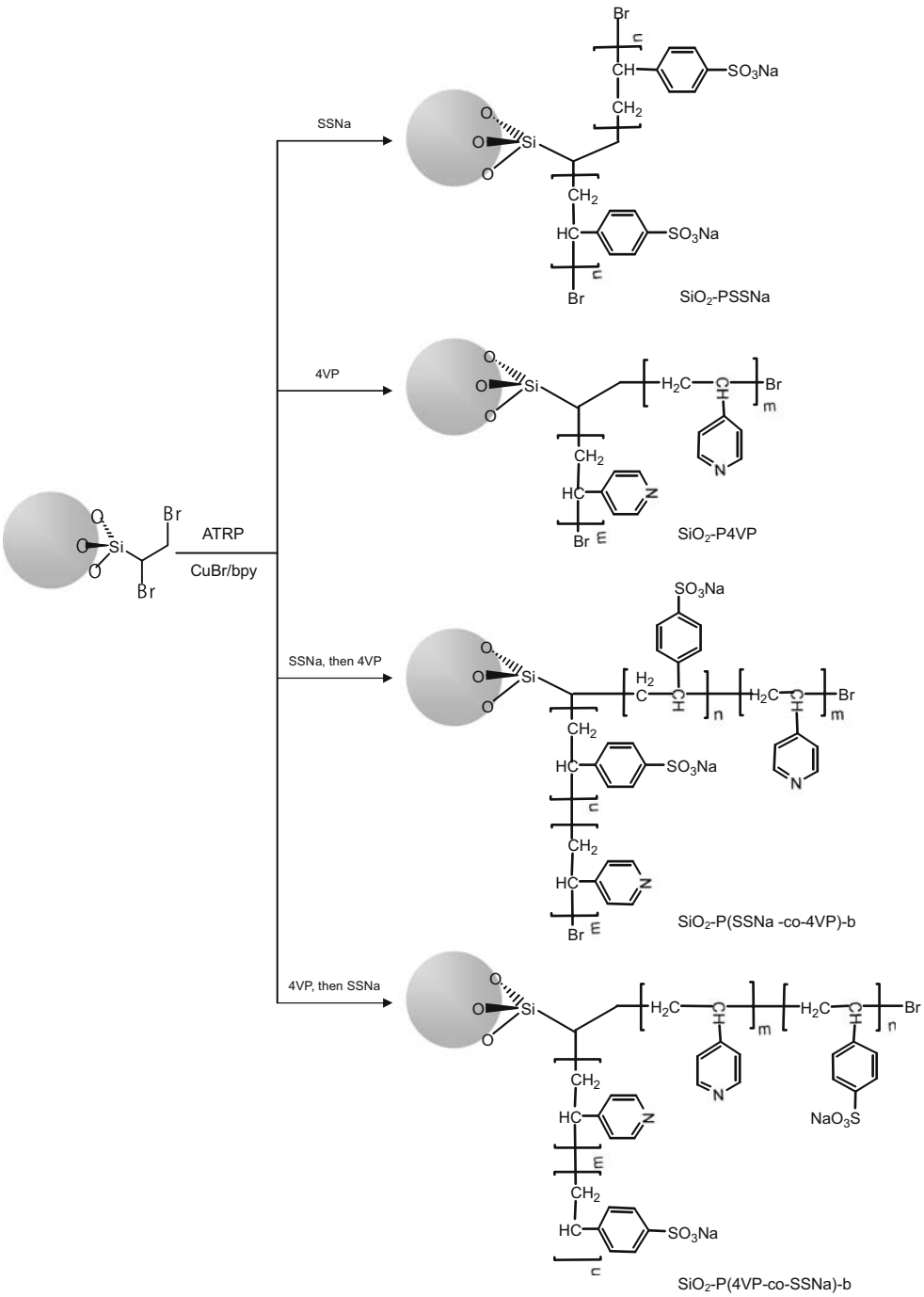

Scheme 1 The schematic of developing polyelectrolyte oligomeric chains on the silica particle

conductivity of these membranes. It is known that cations (especially Li^+ and H^+) do not exhibit noticeable conductivity in dry polymer electrolyte matrixes, but inclusion of a certain amount of solvent into the corresponding matrix will dramatically ease the transport confinement [23]. The study revealed that the pendant polymer chains help accelerating motions of ions in the dispersion medium toward the respective electrodes. It was also perceived that such an assisting role was affected by the solvating extent of the pendant polymer chains. In short, this work attempts to understand the prior-mentioned properties of the polyelectrolyte oligomers that have homo- or di-block (with opposite charges) dense chains anchored on microsilica particles.

Experimental

Materials

Tetraethyl orthosilicate (TEOS; Fluka; >98.0%) and triethoxyvinylsilicane (TEVS; Aldrich; >97%), ammonia (Merck; 25%), cetyltrimethyl ammonium chloride (CTACl; Aldrich; 25% solution in water), bromine (Mallinckrodt, AR®), copper (I) bromide (Aldrich; 98%), sodium 4-styrenesulfonate (Aldrich), and 4-vinylpyridine (Aldrich; 95%), 2, 2′-bipyridyl (Fluka; ≥99%) were used as received.

Synthesis of 1, 2-di-bromoethyl pendant group on silica microspheres

A given amount of aqueous solution (10 ml, 25%) of cetyltrimethyl ammonium chloride, deionized (DI) water (15 ml), and pure methanol (10 ml) were added into a 100-ml beaker with stirring. After the mixture was converted to a homogenous solution, tetraethyl orthosilicate (6 ml, 98%) and triethoxyvinylsilicane (4 ml, 97%) were added into this solution subsequently. This was followed by introduction of an ammonia solution (3 ml, 25%) dropwise under vigorous stirring into the above solution. The resulting mixture was stirred for 18 h and kept still at 80 °C for 3 days to age the resultant colloidal dispersion. The precipitate was filtrated and washed in a mixed solvent of methanol and hydrochloric acid (HCl; 37%; *v*/*v*=0/1) at 90 °C. This purifying manipulation with the aim to extract CTACl was repeated twice and each washing lasted 24 h. A white vinyl-silica powder was obtained after drying, which was identified, according to elemental analysis, to contain pendant vinyl group of 8.3 mmol/g. A given amount of the vinyl-silica powder (0.5 g) was then dispersed in chloroform (5 ml) in a round bottom flask. To the resulting suspension (at 0–5 °C) under vigorous stirring, a bromine solution containing Br_2 of 19.5 mmol in chloroform (Br_2 to $CHCl_3$=1:5 by volume) was slowly dropped in and the addition reaction was completed within 30 min. The brominated vinyl-silica powder was washed three times in chloroform to remove the adsorbed bromine. The brominated powder displays the characteristic infrared (IR) absorption peaks of 1, 2-dibromoethyl group at υ_{C-Br} (567 cm^{-1}) and υ_{C-H} (2,989 cm^{-1}). According to elemental analysis of 1, 2-bromoethyl-SiO_2 powder, the equivalent of R-Br group in the resulting powder was 7.1 mmol/g.

Grafting ionmer chains to 1, 2-di-bromoethyl silica particles through ATRP

In a typical batch of polymerization, the 1, 2-bromoethyl-SiO_2 powder (0.15 g, approximately 1.1 mmol R-Br) was dispersed in a water/methanol mixture (12 ml, *v*/*v*=3:1). SSNa (0.5 g, 2.4 mmol) and 2, 2′-bipyridyl (0.03 g, 0.2 mmol) were then added into this dispersion. The mixture was purged by N_2 for 30 min with continuous stirring at temperature 35–40 °C, and then CuBr (0.06 g, 0.4 mmol) was introduced into the dispersion. The reaction mixture was stirred for 4 h and quenched by air. The blue sediment was washed in doubly Millipore water and centrifuged at 6,000 rpm for 15 min. This purifying procedure was repeated three times to clean up the catalyst residues as well as the monomer left from the PSSNa-grafted silica particles. In the case of constructing the pendant diblock P(SSNa-co-4VP)-b copolymer chains, 4VP was added to the ATRP system where SiO_2-P(SSNa)-Br macroinitiator had been formed in advance, and the subsequent polymerization was carried out in the next 4 h. As to the chain composition, a molar ratio of SSNa/4VP=3/2 in the monomer feed was set. Similarly, the sequence of these two blocks was swapped by introducing 4VP first and then SSNa into the ATRP system to obtain the pendant P(4VP-co-SSNa)-b diblock copolymer chains. The samples synthesized are listed in Table 1.

Instrumental characterizations

The infrared spectra of the grafted silica powders obtained from the three synthetic stages were recorded on a spectrophotometer (Bio-Rad FTIR model 400). The bromination extent of vinyl-silica powder was determined by both elemental analysis (PE 2400 Series II CHN analyzer from Perkin-Elmer) and energy dispersive X-ray (EDX) scanning (JGM-6700F from JEOL). The images of core-shell structure

Table 1 The composition of the grafted SiO_2 particles

Sample	Average molecular weight (Da)	Ratio of composition SSANa to 4VP
SiO_2-PSSNa	1,323	–
SiO_2-P(SSNa-co-4VP)-b	1,015	2:9
SiO_2-P(4VP-co-SSNa)-b	1,050	1:3
SiO_2-P4VP	1,294	–

of the polyelectrolyte-silica microspheres were taken on a transmission electron microscopy (TEM) instrument at 200 kV (JEM-2010). The glass transition behaviors of the grafted polymer layer on silica particles were recorded on a differential scanning calorimetry (DSC) set (Mettler Toledo DSC 822e) using heating rate of 10 °C/min. In order to remove chain motion barriers left behind by different sample preparation histories, all of the samples were scanned from room temperature to 100 °C and cooled down to −20 °C at the same rate. The second scan from this standardized state resulted in a series of energy–temperature diagrams, respectively, which were used for thermal analysis. The influence of pH or the solvent polarity of the dispersion medium on the hydrodynamic dimension of the samples was investigated by dynamic light scattering (DLS; Brookhaven Instruments 90 Plus particle size analyzer). The variation of interfacial charge, with the change of pH, due to the presence of the grafted ionmer layer was investigated by zeta potential measurement (BIC Zetaplus zeta potential analyzer). For DLS and zeta potential analysis, the colloidal dispersions were prepared by the procedure: a particle sample (~3 mg) was dispersed in 6 ml aqueous solution with the aid of ultrasonication for 10 min. The pH solution was adjusted by addition of either NaOH or HCl.

Measurements of molecular weight of the grafted polymer chains

The four grafted samples (approximately 100 mg) were dispersed in 1 ml aqueous HF (5%), and the suspension was stirred at room temperature for 4 h to allow dissolving the silica core. The grafted polymer chains from the disbanded particles became soluble in the HF solution. The resulting polymer solution was then diluted ten times by water and sent for the measurement of molecular weight by gel permeation chromatography (GPC). The GPC analysis (Waters 1515) used water as eluent (flow rate=1.0 ml/min at 25 °C) and the polyethylene glycol calibration standard for the determining of molecular weight of the polyelectrolyte chains.

Measurement of the ionic conductivity in the colloidal dispersions

The samples of polymer-grafted particles (Table 1) were dispersed respectively in aqueous solution of HCl (pH=3) with the aid of ultrasonication to form a colloidal dispersion. Each dispersion was designed to have the solid content of 1 mg/ml (equivalent to approximately 0.01 vol. %) and transferred into a curette (1×1×4 cm) installed with two stainless steel electrodes. The electric conductivity of each suspension was measured using the electrochemical analyzer (Autolab Instrument, frequency scanning range 1 Hz–100 kHz). Similarly, the other set of colloidal suspensions was prepared by using a binary mixture, *N*, *N*'-dimethyl foramide (DMF) and DI water, as the dispersing medium. With respect to a particular powder, the ratio of DMF to water was also varied but the solid content was maintained the unchanged.

Results and discussions

Implantation of ATRP initiating sites to SiO_2 particle

When the sol–gel reaction of TEOS and TEVS took place together inside microspherical droplets surrounded by surfactant molecules, CTACl, the vinyl-SiO_2 microsphere was generated and its TEM image showed that the particle had a dense core and a rather porous thick shell wall surrounding the core (Fig. 1a,b). The porous shell was generated because

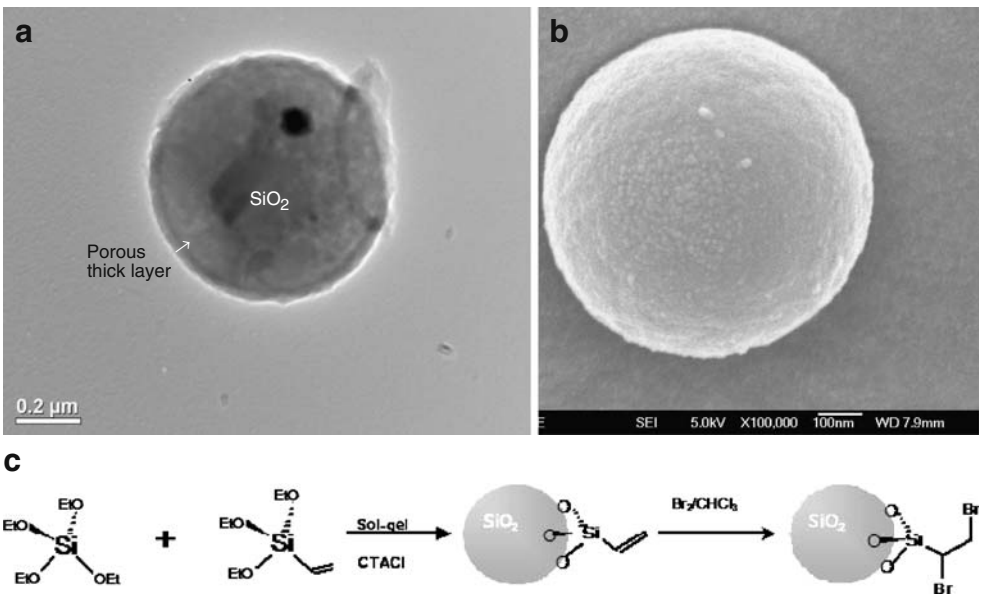

Fig. 1 **a** TEM image of vinyl-silica particle, **b** field-emission SEM image of vinyl-silica particle, and **c** the schematic of forming 1, 2-dibromoethyl-silica particle

it consists primarily of vinylsilane [(–O–)$_3$Si-CH=CH$_2$] units (Fig. 1c), which is caused by the discrepancy in the reactivity between TEVS and TEOS, the former one being far less reactive than the latter one to undertake sol–gel reaction [24] and, therefore, the major portion of TEVS was used to constitute the outer layer of the microsphere.

According to elemental analysis of SiO_2-vinyl particles, the molar ratio of pendant vinyl group to silicon was about 0.4, and about 70% of the vinyl groups were brominated to form 1, 2-dibromoethyl groups according to the EDX surface analysis (Fig. 2). For the liquid phase ATRP, α-bromoalkyl acetate (AcOCR'RBr) is conventionally adopted as the initiator, and some recent reports [25, 26] showed that the initiator could be anchored to a solid substrate through alkoxylcarbonyl (-OCOCHRBr) linkage and therefore polymer chains could be grown from the surface-fastened α-bromoalkyl acetate groups. Compared with this traditional initiator, the pendant 1, 2-dibromoethyl initiator, which we developed in this work, leads to carbon–carbon bond but rather oxygen–carbon bond linkage between the initiator and the solid substrate. The carbon–carbon linkage is intact in an acidic or alkaline medium.

The structural characteristics of the rigid core-soft shell microsphere

Our study found that the maximum molar ratio of monomer to the catalyst [Cu(I)] in the feed of ATRP was about 6 and a higher ratio did not help increase the grafted chain length furthermore. Therefore, this ratio was employed to develop both homopolymer and diblock copolymer chains (Table 1). The generation of short chains was likely due to the entanglement among the growing polymer chains in the porous shell layer of individual SiO_2 microsphere, on which the growing chains were rather cramped with the distending of polymerization. The chain propagating sites became more and more difficult to access by monomers in the liquid phase. The similar phenomenon has also been reported recently [19], in which Chen et al. observed that the PSSNa-grafted silica particle had a relatively weak salt dependence and used it as an evidence of the low molecular weight of PSSNa chains. The above inference of oligomerization could be verified by the TEM image of the PSSNa-SiO_2 particle (Fig. 3), which exhibited an expanded layer and an irregular core contour in contrast to its precursor as shown in Fig. 1a. This morphology can be rationally attributed to the growth of oligomeric PSSNa chains on and underneath the surface of the particle, and as a result, the oligomeric chains expanded the [(–O–)$_3$Si-R] shell layer. As noted above, growing diblock copolymer chains on silica microsphere is the other unique feature of ATRP. In this work, two types of diblock copolymer chains, P(SSNa-co-4VP)-b and P(4VP-co-SSNa)-b, were realized, where suffix "-b" stands for the block type of copolymer. The P4VP block bears positive charges in an acidic medium because each 4VP unit is a proton acceptor, while PSSNa block carries negative charges in a neutral and weak alkaline aquatic medium. The IR spectrum of the SiO_2-P(SSNa-co-4VP)-b (Fig. 4) is taken as an example to show the presence of both the 4VP and SSNa units.

The unique response of the pendant polyelectrolyte short chains to thermal stimulus

Thermal analysis of the grafted oligomeric chains is an effective way to probe the particular polymer chain–chain interactions on the surface of SiO_2 beads. On the DSC diagram of SiO_2-vinyl particles, an endothermic peak emerged at 138 °C (Fig. 5); it can be attributed to the creeping of the porous silica network. Besides this reference sample, an unbound homopolymer sample, PSSNa ($\overline{M_n} \sim 10^4$), was the other reference used, which displays a steep glass transition (T_g) peak consisting of two slopes at 106 °C and 153 °C, respectively. Compared

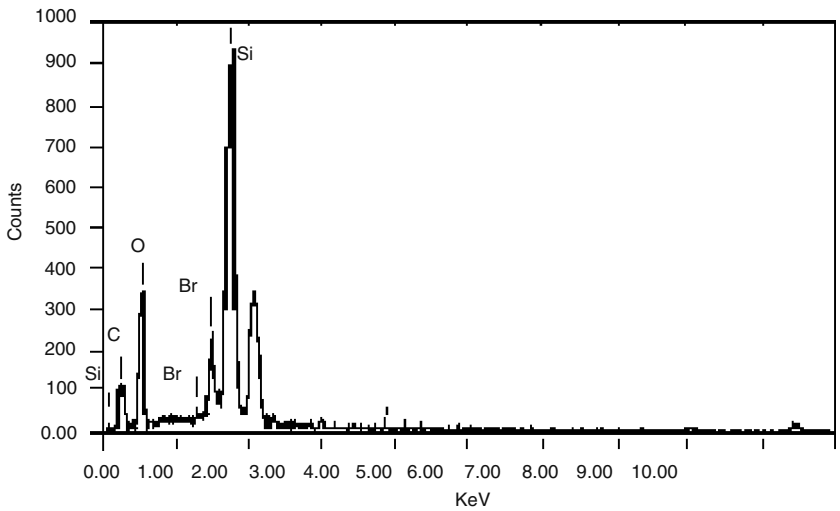

Fig. 2 Energy dispersive spectrum of the brominated silica particles

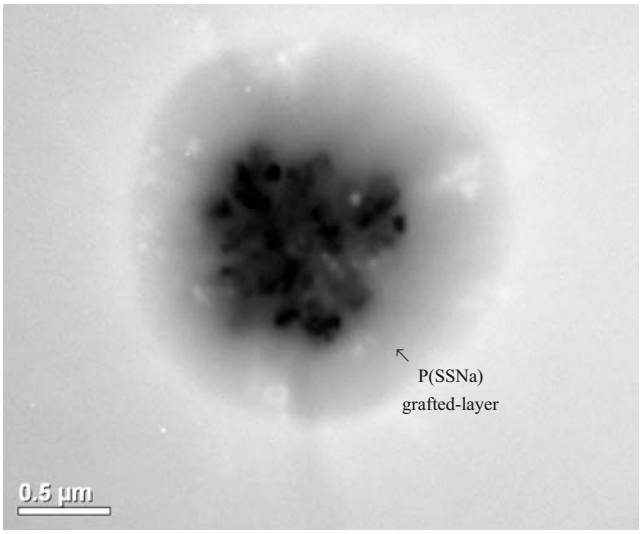

Fig. 3 Transmission electron micrograph of a PSSNa-grafted silica particle

with the DSC profile of polystyrene, the presence of para-substituted sulfonate group in benzene ring increased T_g of the segment motions (from approximately 104±2 °C to 106–139 °C). This strong polar association of sulfonate groups provokes an energy barrier appearing at 153 °C. Furthermore, the bound oligomeric PSSNa chains on silica particles revealed a higher segment motion barrier whose T_g appears at 123 °C in contrast to the foregoing 106 °C for the unbound PSSNa chains because most of the oligomeric chains are implanted in the rather stiff outer shell network, [(–O–)$_3$Si-R], and this constraint environment also promotes the sulfonate group association, which shifts the onset of the corresponding glass transition temperature from 153 °C to 157 °C (Fig. 6). Alternatively, in view of the DSC diagram of SiO_2-P4VP, it exhibited an endothermic peak at 138 °C and a shallow glass transition step at 166 °C, respectively. The first endothermic peak is known as the bulk characteristic of porous silica substrate as found on Fig. 5, whose intensity becomes stronger after ATRP, and the glass transition of the bound P4VP is higher than that of the unbound P4VP polymer that has T_g at 154 °C [27].

The glass transition diagrams of the two pendant diblock copolymer chain structures, SiO_2-P(SSNa-co-4VP)-b and SiO_2-P(4VP-co-SSNa)-b, show very different energy profiles (Fig. 7). For the former type, in which the SSNa blocks were fastened to the silica and the 4VP blocks comprised the outer layer, it displays a rather analogous profile to SiO_2-P4VP. This phenomenon is due to the external location of the compositionally predominant P4VP blocks. On the contrary, for the latter type, it displays an intricate T_g profile, of which the first two endothermic peaks (116 °C and 127 °C) seem to be generated from certain kind of mutual entanglements of the two blocks because neither of these two glass transition peaks resembles their respective homopolymeric forms. This is the result of the external location of PSSNa blocks and of the longer P4VP blocks (Table 1). It also deserves to note that a strong exothermic peak appears at 182 °C, which we assume is the result of temperature-driven complexation of the pendant 4VP groups with sodium ions, which migrate from the PSSNa blocks to P4VP block when the chain motions gain momentum at this temperature.

The impacts of solvating power and pH on the hydrodynamic volume of the hybrid core-shell particles

In this section, we look into how the solvating behavior and surface charge of the hybrid core-shell particles affect their hydrodynamic volume determined by the dynamic light scattering and zeta potential measurements. Figure 8 shows the mean sizes of the particles in the mixture of (H_2O–CH_3OH), which reflect different solvating extents of the grafted oligomeric chains in the dispersion media. For the two types

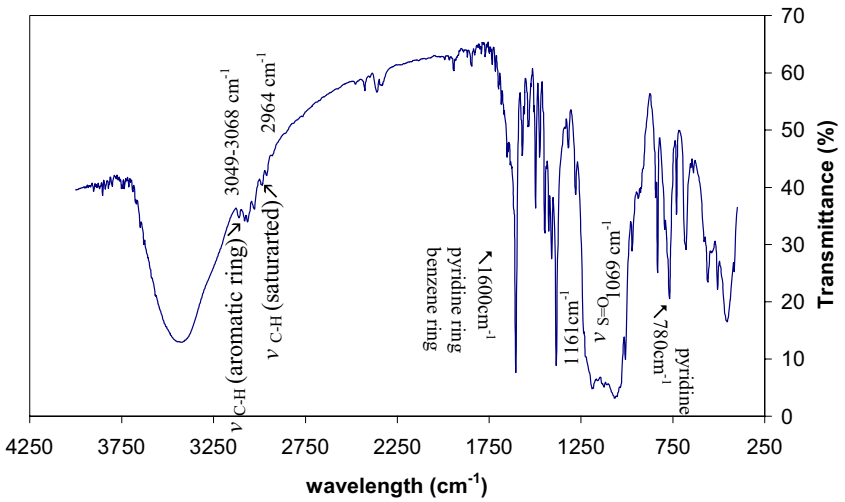

Fig. 4 Fourier transform infrared spectrum of the copolymer-grafted silica particles

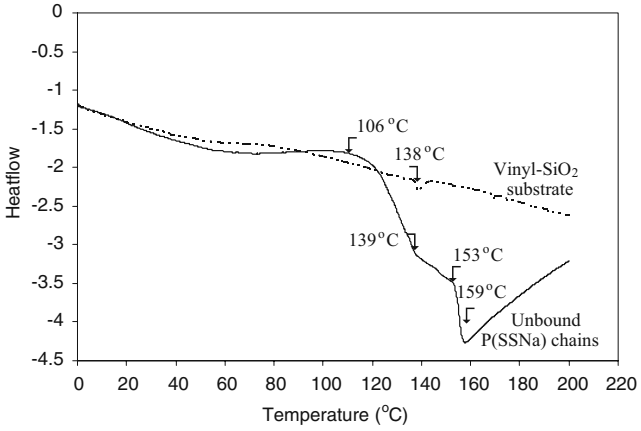

Fig. 5 Differential scanning calorimetric analysis of the unbound PSSNa and vinyl-silica

of homopolymer-grafted particles (inset), SiO_2-P4VP and SiO_2-PSSNa, they exhibited very different response to the increase of methanol mole fraction (x). SiO_2-P4VP particles underwent a quick contraction in the range from pure water to x=0.2, while SiO_2-PSSNa particles underwent a persistent contraction till x=0.5. A certain portion of the pendant 4VP groups may be protonated in water (pH=6.4) to form pyridinium and, therefore, the repulsive interactions of positive pyridinium groups sustain the maximum particle sizes of SiO_2-P4VP. But the partially protonated P4VP chains quickly exhibited lyophobic tendency with a slight increase in the content of methanol in the dispersion medium. According to the above comparison, the bound PSSNa chains are better solvated in the binary solvent than the bound P4VP chains due to the strongly hydrophilic nature of sulfonate groups. Nevertheless, with inspecting the two copolymers, we found that, in contrast to the exteriorly located PSSNa blocks, the exteriorly located P4VP blocks favored solvating of the polymer layer. This result implies that solvating of the inner blocks could mount the solvating extent of outer blocks. In

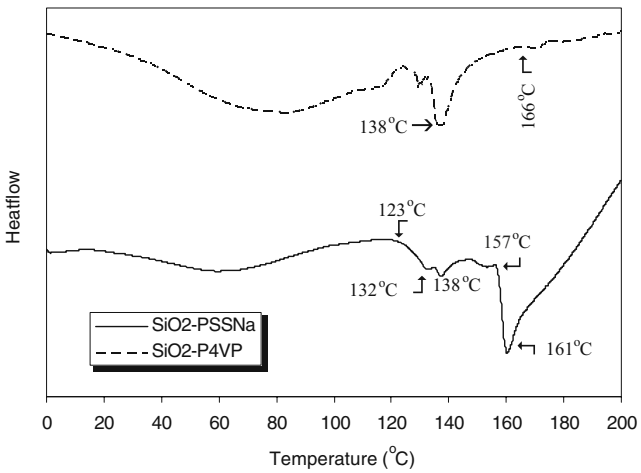

Fig. 6 DSC analysis of the PSSNa- and P4VP-grafted silica particles

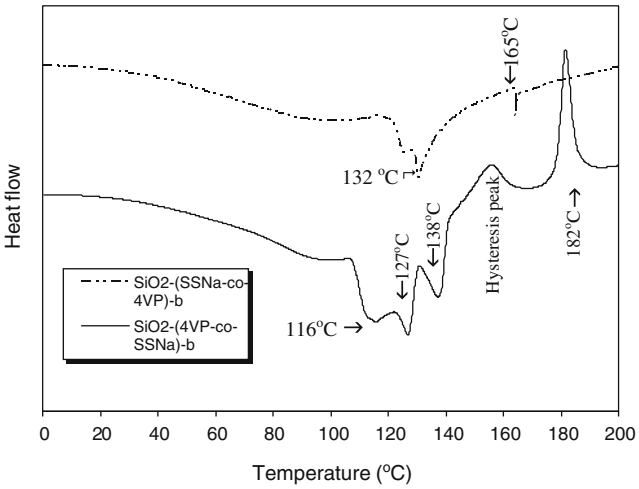

Fig. 7 DSC analysis of the P(SSNa-co-4VP)-b and P(4VP-co-SSNa)-b grafted silica particles

other words, a lyophilic internal layer could enhance affinity of the external lyophobic blocks for the dispersion medium.

With respect to the zeta potential measurement of the two homopolymer-grafted types of particles (Fig. 9), as expected, SiO_2-P4VP exhibited positive ζ potential in aqueous medium with pH≈6.4 because of the protonation as aforementioned, whereas the system exhibited negative ζ potential when pH>6.4, which implies the occurrence of OH^- ion adsorption to the outmost pendant 4VP groups. The adsorption incurs a negatively charged slip plane of fluid [28] that moves as a part with the particle, which was sensed by ζ potential measurement. On the other hand, SiO_2-PSSNa exhibited negative ζ potentials at pH values above its iso-

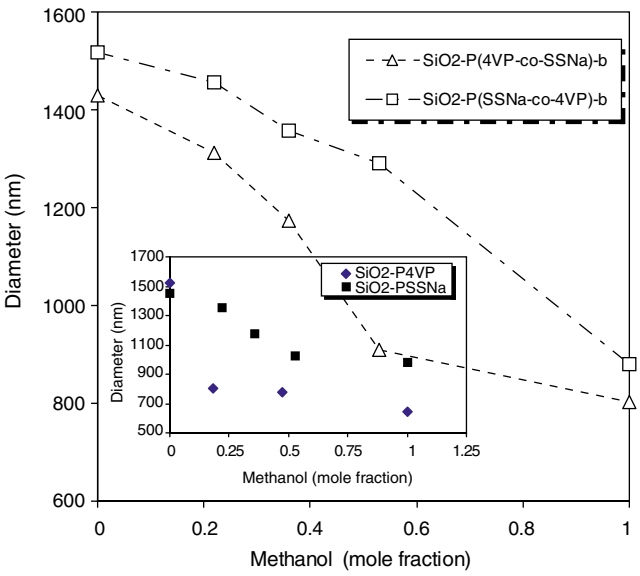

Fig. 8 Variation of the mean dynamic diameter of P(SSNa-co-4VP)-b and P(4VP-co-SSNa)-b grafted silica particles with the methanol content in the aqueous dispersion medium. *Inset* represents PSSNa- and P4VP-grafted silica particles

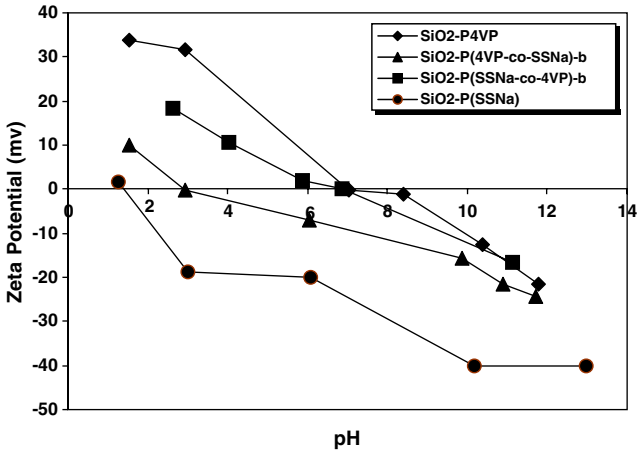

Fig. 9 Influence of pH on zeta potential of polymer-grafted silica particles in aqueous solution

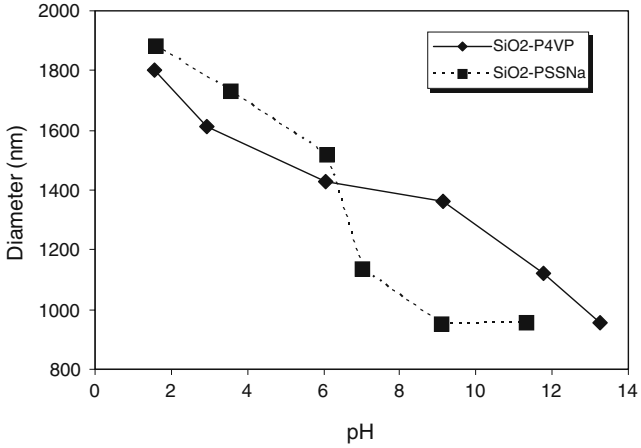

Fig. 10 Influence of pH on the mean dynamic diameter of PSSNa- and P4VP-grafted silica particles

electric point (IEP) that happens at pH=1.3 because the sulfonic acid is strongly acidic. Hence, the slip layer of fluid in this case would be formed by the outmost sulfonate groups and hydrated water molecules. Similar ATRP brush particle systems have been previously investigated by Percy et al. and Fulghum et al. [9, 29]. In light of the relation of ζ potential vs. pH of the two copolymer-grafted particles, the phenomenon of partial charge neutralization between the two blocks was observed. For SiO_2-P(4VP-co-SSNa)-b particles, despite possessing a negatively charged outer PSSNa layer, its IEP occurs at almost pH=3 and, hence, its ζ–pH curve located quite above that of SiO_2-PSSNa in Fig. 9. On the other hand, SiO_2-P(SSNa-co-4VP)-b particles possess a thick P4VP outer layer and, thus, show almost the same IEP as SiO_2-P4VP, but its ζ–pH curve still located beneath that of the SiO_2-P4VP curve due to the partial charge neutralization effect of the negatively charged inner layer. The charge neutralization is in principle driven by the softness of chains in the dispersion liquid medium.

The DLS–pH curve of the dispersion of SiO_2-PSSNa particles in aqueous solution shows that the hydrodynamic volume of particles undergo shrinking with increasing pH (Fig. 10) and a steep decreasing happens in the range pH=6.0–6.5. Being a strong polyelectrolyte, as seen from the ζ potential measurement of SiO_2-PSSNa in aqueous solution, the polymer chains bear negatively charged sulfonate groups and the charge density increases with increasing pH. At the same time, the counter-ion layer composed primarily of Na^+ ions becomes thicker correspondingly. The observed reducing trend of hydrodynamic volume could be interpreted as the compressing effect of the counter-ion layer. In comparison with this, P(4VP-co-SSNa)-b particles show relatively slower size-contraction trend because of the buffering effect of the inner P4VP segments. This is particularly obvious in the basic medium. For instance, the DLS size of P(4VP-co-SSNa)-b is approximately 1,350 nm while that of SiO_2-PSSNa is down to approximately 950 nm at pH=9 even though the latter one has a slightly larger size than the former one at pH=1. The buffering effect as mentioned is deemed to cause by the move of some inner P4VP blocks into the outer PSSNa layer because of their flexibility in hydrated state. Alternatively, SiO_2-P4VP particles also underwent contraction with the increase in pH of the dispersion medium due to the decrease of the pyridinium groups. The mounting effect of inner layer also happens in the P(SSNa-co-4VP)-b particle as presented in Fig. 11.

The role of the grafted polymer chains in assisting with ion transport

Whether or not and how the polymer chains grafted to SiO_2 microspheres could assist ion transport in a liquid medium where they are dispersed is an appealing problem to study. As indicated in "Measurement of the ionic conductivity in the colloidal dispersions" section, the dispersion was designed to have a substantially low volume fraction of the

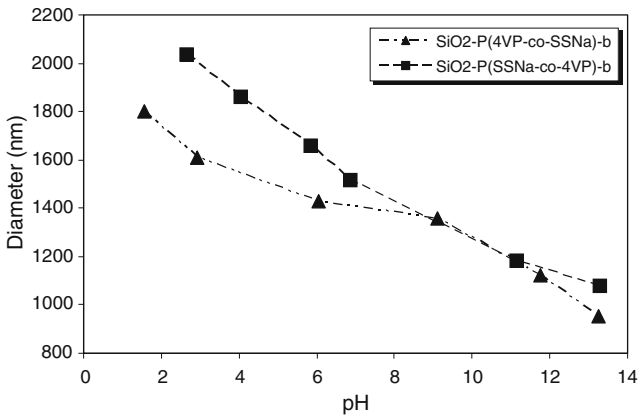

Fig. 11 Influence of pH on the mean dynamic diameter of P(SSNa-co-4VP)-b and P(4VP-co-SSNa)-b grafted silica particles

particles (~1.0×10^{-2}%), but this solid content is equivalent to about 10^9 particles moving about in 1 cm^3 liquid dispersion medium, which means on average, a particle could be found in per 10^3 μm^3 space. At this low occupancy level, we examined how the pendant polymer chains acted on escalating ionic conduction in the liquid phase. Figure 12 displays proton conductivity of the colloidal dispersions of which the dispersion medium is an aqueous solution of HCl (pH=3). The pendant sulfonic acid groups promote proton transport, while the pendant 4VP groups, being an organic base, retard proton conduction. Regarding the copolymer arms, although P(4VP-co-SSNa)-b chains are less expanding (or solvated) than P(SSNa-co-4VP)-b in aqueous solution with pH=3 (Fig. 11), the former one revealed stronger role in facilitating proton transport because of their exterior PSSNa blocks. The observation suggests that the surface layers of these floating particles, despite substantially low space occupancy, could confer an alternative proton-conducting channel wherein protons undertake faster hopping than in the bulk phase of solution.

We further examined the ionic conductivity of the colloidal dispersion formed by dispersing the particles in DMF–water mixture (Fig. 13). This test involved three types of particles containing PSSNa blocks. The concentration of sodium ion, as the major charge carrier, in the resulting colloidal dispersions followed the order: SiO_2-PSSNa>SiO_2-P(4VP-co-SSNa)-b≈SiO_2-P(SSNa-co-4VP)-b, because each dispersion system contained the same amount of particles but each type of the particles possessed different contents of PSSNa as listed in Table 1. The resulting dispersions in DMF–H_2O mixtures were very stable regardless of the ratio of DMF to H_2O. The dispersions of SiO_2-PSSNa exhibited the highest ionic conductivity and the conductivity increased with the reducing of DMF portion due to its highest Na^+ concentration among the three and the fact that ionization dissociation of the SSNa groups becomes stronger with increasing of water content. However, it is noteworthy that the unique observation comes from the differences between the two grafted copolymer types of particles, SiO_2-P(4VP-co-SSNa)-b and

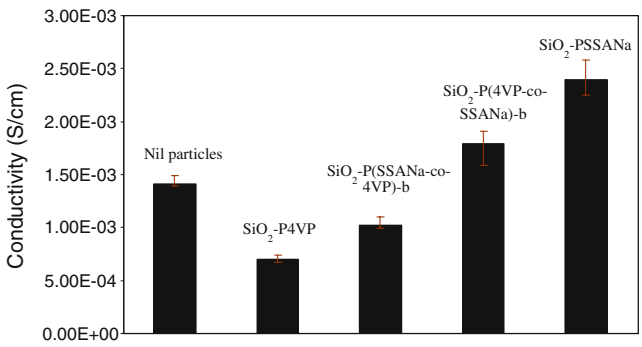

Fig. 12 Conductivity of the acidified water (pH=3) loading different particles

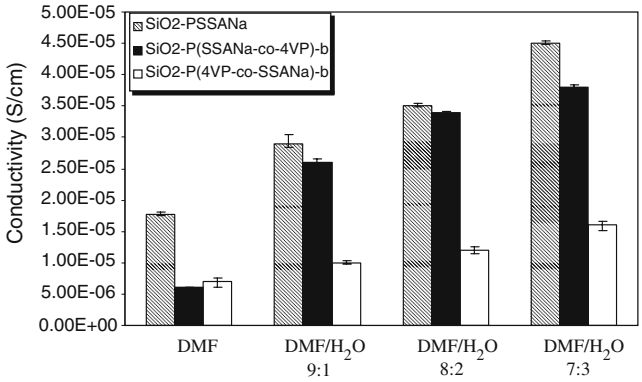

Fig. 13 Conductivity of different ration DMF and water solution loading different particles

SiO_2-P(SSNa-co-4VP)-b. Of the two, the former one contains the exteriorly located PSSNa blocks. Hence, it is supposed to be able to reveal higher ionic conductivity than the latter one. The measurement results yet were different from this prediction. The dispersion of the SiO_2-P(SSNa-co-4VP)-b particles showed a clear increasing trend of sodium ion conductivity with increasing of water content in the dispersion medium. We are inclined to consider that the swelling of the P4VP block in DMF-H_2O mixtures as well as the weak association between Na^+ ion and 4VP nitrogen play important roles in channeling transport of Na^+ ions. This association [30] is regarded to have a weak strength so that the migration of Na^+ ions is not hindered. It deserves to note that the Na^+ conductivity of this system jumps by five times from pure DMF to DMF–H_2O (v/v=9), whereas the dispersion of SiO_2-PSSNa conferred only a three-time increase in Na^+ conductivity in response to the same variation of the water content. The inner PSSNa block functions like a switch, whose hydration triggers a clear ionic conductivity leap. On the contrary, SiO_2-P(4VP-co-SSNa)-b particles displayed only a slim superiority over SiO_2-P(SSNa-co-4VP)-b particles in pure DMF. The outer PSSNa layer, albeit it swells better with in-creasing of water content in the DMF–H_2O mixtures, prevents the P4VP inner layer from acting as effective as the outer P4VP layer to channel transport of sodium ions. In brief, the sequence of the two blocks has a clear impact on sodium ion conduction, namely the inner PSSNa placement is superior over its outer placement because P4VP blocks take part in shipping Na^+ ions when they are exposed to liquid phase.

Conclusion

In this work, a specific structure of microsphere, comprising a silica core and a densely grafted hydrophilic polymer layer with low molecular weights, was synthesized by carrying out the atom transfer radical polymerization of 4-styrenesulfonate and 4-vinylpyridine. Thus, four types of grafted chain struc-

tures were achieved: two homopolymers and two block copolymers with inverted block sequence. These four types of hairy microspheres exhibit different solvating volumes (hydrodynamic volumes) in methanol–H_2O mixtures with different ratios of the two components and in aqueous solution with different pH values, respectively. These variations are governed by solvating extent and charge repulsion or neutralization in the grafted polymer layers. Besides these two factors, the new insight gained from this study is the leverage of the inner blocks of copolymer on the magnitude of surface charge and hydrodynamic volumes of the particles in a dispersion medium. Furthermore, the study also examined whether or not the grafted polymer chains could assist with ion transport in the liquid medium where a substantially low portion of particles is dispersed. In the acidic medium, the results showed that the grafted PSSNa chains facilitate but the grafted P4VP chains retard proton transport and the copolymer layer bearing the exterior PSSNa blocks offers a stronger promoting action than that with the PSSNa inner blocks. The investigation was extended to DMF–H_2O dispersion medium, where Na^+ from PSSNa became the major charge carrier. An obvious cooperative action between the inner PSSNa blocks and the outer P4VP blocks to strongly propel Na^+ conduction was observed in DMF–H_2O (v/v=9), while the reversed block sequence did not present such an assisting role in the same dispersion system.

References

1. Coad BR, Steels BM, Kizhakkedathu JN, Brooks DE, Haynes CA (2006) Biotechnol Bioeng 97:574 doi:10.1002/bit.21283
2. Pallandre A, Lambert B, Attia R, Jonas AM, Viovy JL (2006) Electrophoresis 27:584 doi:10.1002/elps.200500761
3. Padeste C, Farquet P, Potzner C, Solak HH (2006) J Biomater Sci Polym Ed 17:1285 doi:10.1163/156856206778667505
4. Midha S, Torgerson PM, Hall C, US 5565193
5. Rong MZ, Zhang MQ, Zheng YX, Zeng HM, Walter R, Friedrich K (2001) Polymer 42:167 doi:10.1016/S0032-3861(00)00325-6
6. Matyjaszewski K, Xia J (2001) Atom transfer radical polymerization. Chem Rev 101:2921–2990 doi:10.1021/cr940534g
7. Werne T, Patten TE (1999) J Am Chem Soc 121:7409 doi:10.1021/ja9911081
8. Werne T, Patten TE (2001) J Am Chem Soc 123:7497 doi:10.1021/ja010235q
9. Percy MJ, Michailidou V, Armes SP (2003) Langmuir 19:2072 doi:10.1021/la020794q
10. Gu B, Sen A (2002) Macromolecues 35:8913 doi:10.1021/ma020809r
11. Pyun J, Jia SJ, Kowalewski T, Patterson GD, Matyjaszewski K (2003) Macromolecules 36:5094 doi:10.1021/ma034188t
12. Zheng G, Stover HDH (2002) Macromolecules 35:6828 doi:10.1021/ma0121464
13. Ohno K, Koh K, Tsujii Y, Fukuda T (2002) Macromolecules 35:8989 doi:10.1021/ma0209491
14. Zhao B, Brittain WJ, Zhou W, Cheng SZD (2000) Macromolecules 33:8821 doi:10.1021/ma000434e
15. Pantoustier N, Moins S, Wautier M, Degee P, Dubois P (2003) Chem Commun 2:340 doi:10.1039/b208703k
16. Duracher D, Sauzedde F, Elaissari A, Pichot C, Nabzar L (1998) Colloid Polymer Sci 276:920 doi:10.1007/s003960050329
17. Senff H, Richtering W (1999) Langmuir 15:102 doi:10.1021/la980979q
18. Senff H, Richtering W (1999) J Chem Phys 111:1705 doi:10.1063/1.479430
19. Chen XY, Randall DP, Perruchot C, Watts JF, Patten TE, Werne T, Armes SP (2003) J Colloid Interface Sci 257:56 doi:10.1016/S0021-9797(02)00014-0
20. Feng X, Liu Y, Lu C, Hou W, Zhou J-J (2006) Nanotechnology 17:3578 doi:10.1088/0957-4484/17/14/037
21. Hariharan R, Biver C, Russel WB (1998) Macromolecules 31:7514 doi:10.1021/ma9718199
22. Hariharan R, Biver C, Mays J, Russel WB (1998) Macromolecules 31:7506 doi:10.1021/ma971818g
23. Stolwijk NA, Obeidi S (2005) Diffusion in materials: DIMAT 2004, PT 1 AND 2 237–240:1004
24. Brickner CJ, Scherer G (1990) Sol–gel science: the physics and chemistry of sol–gel processing. Academic, San Diego, p 135
25. Liu TQ, Jia SJ, Kowalewski T, Matyjaszewski K, Casado-Portilla R, Belmont J (2003) Langmuir 19:6342 doi:10.1021/la034219d
26. Mori H, Seng DC, Zhang MF, Muller AHE (2002) Langmuir 18:3682 doi:10.1021/la011630x
27. Jian W, Cheung MK, Mia Y (2001) Polymer 42:3087 doi:10.1016/S0032-3861(00)00643-1
28. Cao G (2004) Nanostructures & nanomaterials: synthesis, properties & applications. Imperial College Press, London, p 153
29. Fulghum TM, Patton DL, Advincula RC (2006) Langmuir 22:8397 doi:10.1021/la0601509
30. Gapeev A, Dunbar RC (2003) Int J Mass Spectrom 228:825 doi:10.1016/S1387-3806(03)00242-2